COBEM 2023 27TH INTERNATIONAL CONGRESS OF MECHANICAL ENGENEERING

ABCM Brazilian Society of Mechanical Sciences and Engineering
27th ABCM International Congress of Mechanical Engineering
December 04-08, 2023, Florianópolis-SC, Brazil

COB-2023-1826
VIBRATION REDUCTION OF FLEXIBLE SHAFT WITH ACTIVE BEARING

Heitor Antônio Pereira da Silva
Rodrigo Nicoletti
University of São Paulo, School of Engineering of São Carlos, Trabalhador São Carlense 400, 13566-590, São Carlos, SP, Brazil
heitorantonio@usp.br, rnicolet@sc.usp.br

Abstract. *Large rotating machines are essential elements in the production chain, but they may occasionally operate under unpredicted or off-the-norm conditions, resulting in failures and significant economic losses. To minimize the consequences of non-standard operations, it is possible to change the characteristics of the bearings that support the rotor. However, with conventional bearings, this is only possible by completely stopping the machine, which also results in economic losses. The solution comes from the development of active bearings, which allow the modification of the dynamic characteristics of the machine during operation, without needing machine stops. The goal of this work is to utilize a PD (Proportional-Derivative) controller in a system consisting of a long and flexible shaft with a central disk mass. The shaft is supported by bearings on one end and an active bearing on the other. Two cases will be examined: the first is to control the vibration amplitude of the shaft at the end where the active tilting pad journal bearing is located, while the second is to control the vibration amplitude on the disk. This approach aims to reduce friction and wear on rotating machines, thereby extending their useful life, ensuring reliable operation, and minimizing economic losses. The development of active bearings is a significant industry innovation, with positive impacts on the efficiency and profitability of operations that depend on this equipment.*

Keywords: *Active TPJB, Electromagnetic Actuators, Control, Flexible Shaft.*

1. INTRODUCTION

Rotating machines play a crucial role in the production chain, from the extraction and supply of raw materials (such as mining, agriculture, and energy generation) to the manufacturing industry (chemical, food, machinery, equipment, and vehicles), and ultimately reaching consumers as finished products (home appliances, electronics, computer drives, etc.). Considering the wide range of applications of rotating machines, their importance in the production system can be inferred, as well as the economic consequences of using more efficient and less polluting machinery (Nicoletti, 2013). Therefore, the design of large-scale rotating machines, such as gas turbines, steam turbines, and compressors, must meet requirements of efficiency, energy consumption, reliability, and component lifespan, which are equally important.

In the past, various ideas emerged to actively control vibrations in rotating systems using magnetic bearings. These bearings have the advantage of operating without physical contact, covering a wide frequency range, and are considered clean systems as they do not require lubricating fluids, except for air (Bleuler *et al.*, 2009). However, the use of magnetic bearings becomes prohibitively expensive when applied to large-scale rotating systems. In such applications, the forces involved are high, and the magnetic system becomes complex and bulky. Additionally, protective systems, such as auxiliary bearings, must be added to the machine to address potential failures in the electrical system or overloading of the magnetic bearing. Therefore, magnetic bearings alone are not the most suitable option for large-scale rotating machinery.

From this perspective, the concept of a segmented hydrodynamic bearing with electromagnetic actuators mounted on the bearing shoes was developed. This concept aims to combine the advantages of segmented and magnetic bearings to modify the dynamic characteristics of the bearing in an integrated manner within a single machine system. In this approach, the goal is to leverage the load-bearing capacity and stability of the segmented hydrodynamic bearing to support the rotor, while the actuation is performed by the magnetic actuators installed on the bearing shoes. By using the segmented bearing as the mechanism for rotor support through hydrodynamic lubrication, it becomes possible to reduce the size of the magnetic actuator since it is now responsible solely for actuation rather than bearing support, as in magnetic bearings. Consequently, there is no need for a safety system in case of magnetic actuator failure since the lubrication assumes the role of rotor support (Pizarro Viveros and Nicoletti, 2014; Moraes and Nicoletti, 2010).

One limitation of this system is related to the increase in the moment of inertia of the bearing shoes due to the insertion of electromagnetic actuators. This occurs because the shoes become larger and heavier due to the presence of the actuators. When the electromagnetic actuator is activated and exerts attractive forces on the rotor towards the shoe, as a reaction, the attractive forces on the shoe also act towards the rotor. However, these actuation forces are not collinear with the pivot point of the shoes, resulting in a torque on the shoe and, consequently, altering its angular position.

As a way to improve the system, the idea of modifying the location of the electromagnetic actuators within the segmented bearing arises. The alternative is to position the electromagnetic actuators in the bearing housing, so that the electromagnetic force acts on the outer face of the pivot pads (segmented hydrodynamic bearing with active segments - Fig. 1). This approach reduces the size and inertia of the pads, returning them to their original size, and the modification of the dynamic characteristics of the rotor-bearing system occurs through the modification of the angular position of the pads. In other words, the actuation and control forces would no longer act on the rotor, but on the pads.

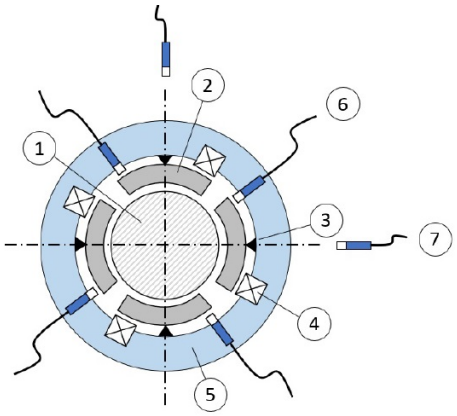

Figure 1. Hydrodynamic bearing with active pads: 1) rotor, 2) pad, 3) pivot, 4) electromagnetic actuators, 5) housing, 6) pad proximity sensor, 7) rotor proximity sensor.

The angular movement of the pad, caused by the electromagnetic actuator, would affect the hydrodynamic pressure distribution in the radial clearance between the pad and the rotor, thereby altering the force balance on the rotor. By adopting an appropriate control strategy, this change in the force balance on the rotor can alter the static and dynamic characteristics of the rotor-bearing system (allowing for system control – Pereira da Silva and Nicoletti (2021)).

The project aims to utilize a previously established mathematical model from previous works to control the vibration amplitude of a flexible shaft with a centrally located known mass disc, subjected to mass imbalance. The objective is to conduct two case studies: the first case involves controlling the vibration amplitude of the shaft within the bearing and directly acting on the bearing itself, resulting in localized control. The second case study focuses on controlling the vibration amplitude of the shaft on the disc, with actuation on the bearing, leading to a displaced control scheme where a simple Proportional-Derivative controller is implemented in the control loop.

This strategy allows for the regulation of the shaft's vibration, ensuring a more stable performance and reducing the undesired effects caused by mass imbalance. The use of a Proportional-Derivative controller provides a fast response to variations in vibration amplitude, allowing for appropriate system adjustments. This simplified approach to the controller enables easier and more accessible implementation, serving as a viable alternative to enhance system performance without the need for complex control techniques.

2. MATHEMATICAL MODELING

The objective of this project is to study the mathematical model of an active hydrodynamic tilting pad journal bearing. This model consists of four pads, actuators positioned behind them, and a flexible shaft with a central disc, as illustrated in the figure below:

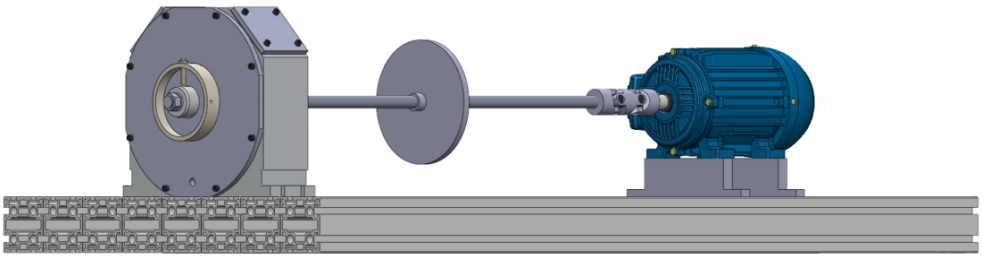

Figure 2. Active hydrodynamic bearing with a flexible shaft and a central disc schematic.

There are several factors taken into consideration in the development of the hydrodynamic model of a tilting pad journal bearing. Initially, the pressure distribution on each pad is determined using the Reynolds equation(Hamrock *et al.*, 2004).

$$\frac{\partial}{\partial y}\left(\frac{h_i^3}{\mu_i}\frac{\partial p_i}{\partial y}\right)+\frac{\partial}{\partial z}\left(\frac{h_i^3}{\mu_i}\frac{\partial p_i}{\partial z}\right)=6U\frac{\partial h_i}{\partial y}+12\frac{\partial h_i}{\partial t} \tag{1}$$

where $p_i(y,z)$ is the pressure distribution on the oil film over the surface of the i-th pad, is obtained using the Reynolds equation, where $h_i(y)$ represents the oil film thickness, which is the distance between the rotor and the i-th pad, and $\mu_i = \mu_i(y,z,T_i)$ is the dynamic viscosity of the oil on the i-th pad. As seen in Eq.(1), the hydrodynamic pressure distribution is directly related to various parameters, with the oil film thickness being one of the key parameters studied in this work.

The oil film thickness along the surface of the i-th pad can be obtained using the expression proposed by Russo (1998). For the bearing with four pads, the expression takes the following form:

$$h_i(y)=R_s-R-[y_r+\alpha_i*(R_s+h_s)]\,\text{sen}\left(\frac{y}{R_s}\right)+(x_r+R_s-R-h_o)\cos\left(\frac{y}{R_s}\right) \tag{2}$$

in this expression, R_s represents the radius of the pad, R is the radius of the rotor, (x_r, y_r) are the coordinates of the rotor, α_i is the angular position of the i-th pad, h_s is the thickness of the pad, and h_o is the nominal radial clearance.

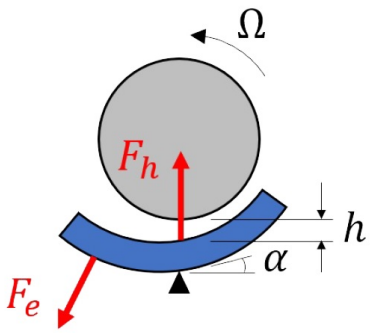

Figure 3. Electromagnetic force acting on the pad and hydrodynamic force acting on the rotor.

In order to determine the dynamic behavior of the shaft, it is necessary to employ the finite element method. The shaft is discretized into multiple elements, and it is crucial to understand the equation of motion that represents this behavior, taking into account the effects of rotation, translation, gyroscopic, stiffness and damping. With that being said, The governing equations of motion for a rotor system, as presented by Nelson and McVaugh (1976), can be expressed as follows:

$$[M]\ddot{u}+[D-\omega G]\dot{u}+[K]u=F(t) \tag{3}$$

Due to the discretization of the shaft, numerous degrees of freedom arise, resulting in a significant increase in simulation time required to determine the dynamic behavior of the system. This becomes excessively costly when implementing control loops in the system. To address this issue, an alternative approach to reduce simulation time was employed: modal reduction of the system. This approach involves considering only a few natural frequencies that approximate the dynamic behavior of the system. The reduction model used in this project is the same as that presented in Nicoletti (2003).

$$[A]\dot{q}+[B]q=\begin{Bmatrix}F(t)\\0\end{Bmatrix} \tag{4}$$

The mathematical model of the electromagnetic actuators is the same as that presented in Pizarro Viveros and Nicoletti (2014). Hence, the electromagnetic force is given by:

$$F_e=\frac{\mathcal{I}}{d^2} \tag{5}$$

where $\mathcal{I}$ is the electric current in the electromagnetic actuator, and d is the distance between the actuator and the back surface of the pad. The electric current in the electromagnet is related to the electric voltage by the expression:

$$\mathcal{I} = \left(\frac{a_0}{\mathrm{i}\omega\, b_1 + b_0} \right) V_{ref}(t) \tag{6}$$

where V_{ref}(t) is the reference electrical voltage applied to the actuator drive. The drive supplies the actuator with electrical voltages ranging from 0 to 24 V for reference voltages between 0 and 10 V, and (a_0, b_1, b_0) are the dynamic parameters of the electromagnetic actuator.

Therefore, knowing the electrical voltage, the resulting current $\mathcal{I}$ is calculated using Eq. (6), and the electromagnetic force F_e is calculated using Eq.(5). This force is applied to the surface of the pad, causing a moment on the pad, as shown in Fig. 3. This moment affects the angular position of the pad, thereby altering the oil film thickness on the pad. The resulting hydrodynamic force is calculated using Eq.(1), and the hydrodynamic force acting on the rotor (Fh - Fig. 3) is obtained.

The equations of motion for the mathematical model of an active hydrodynamic tilting pad journal bearing can be expressed as follows:

$$\begin{cases} I_s \ddot{\alpha}_1 = F_{e1} L_e - F_{ht1} h_s \\ I_s \ddot{\alpha}_2 = F_{e2} L_e - F_{ht2} h_s \\ I_s \ddot{\alpha}_3 = F_{e3} L_e - F_{ht3} h_s \\ I_s \ddot{\alpha}_4 = F_{e4} L_e - F_{ht4} h_s \end{cases} \tag{7}$$

where M_e is the mass of the shaft, F_{hx} and F_{hy} are the resulting hydrodynamic forces acting in the X and Y directions of the shaft, F_X^{unb} and F_Y^{unb} are the unbalanced mass forces applied to the shaft in the X and Y directions, and a_x and a_y represent the positions of the shaft in the X and Y directions.

The control strategy used was a Proportional-Derivative (PD) controller, which can be expressed by the following expression:

$$V_{ref} = G_P e + G_D \dot{e} \tag{8}$$

where V_{ref} is the reference electrical voltage of the drive, G_P and G_D are the proportional and derivative gains of the controller, e is the position error, which is the difference between the controller's reference position and the actual position of the shaft, and $\dot{e}$ is the velocity error.

3. NUMERICAL PROCEDURE

The mathematical model of the active bearing in study was implemented in MATLAB. The equations of motion of the system (Eq.(7)) are integrated in time using the command `ode15s`, which is a variable-step, variable-order (VSVO) solver based on the numerical differentiation formulas (NDFs) of orders 1 to 5, suitable for stiff problems (Shampine and Reichelt, 1997).

Figure 4 presents a flow chart of the algorithm, which can be described by the following steps:

1. input data: bearing geometry, bearing/rotor loading, rotating speed (Ω), initial positions of the rotor and pads $\{X_0\}$, initial velocity of rotor and pads $\left\{\frac{\partial X_0}{\partial t}\right\}$, initial current in the electromagnets $\{\mathcal{I}_0\}$;

2. calculate the thickness of the oil film on the i-th pad. The Finite Difference Method is applied to the Reynolds equation for the i-th pad, where ambient pressure is assumed at the boundary conditions and the Gümbel assumption is used as a cavitation model;

3. calculate the pressure distribution, and consequently the hydrodynamic forces. Steps 2 to 3 are repeated for the other pad;

4. use the resultant hydrodynamic force in the finite element method to determine the position and velocity along the flexible shaft for each discretized element. In order to reduce computational time for the calculations, a modal reduction model is employed, which includes only the first two natural frequencies to represent the behavior of the shaft.

5. obtain the control voltage to be applied to the actuators by adopting a Proportional-Derivative (PD) control strategy. For that, the position and velocity errors are determined from reference (desired) values;

6. determine the distance between each electromagnetic actuator and the respective pad. Calculate the resultant electromagnetic force acting on each pad;

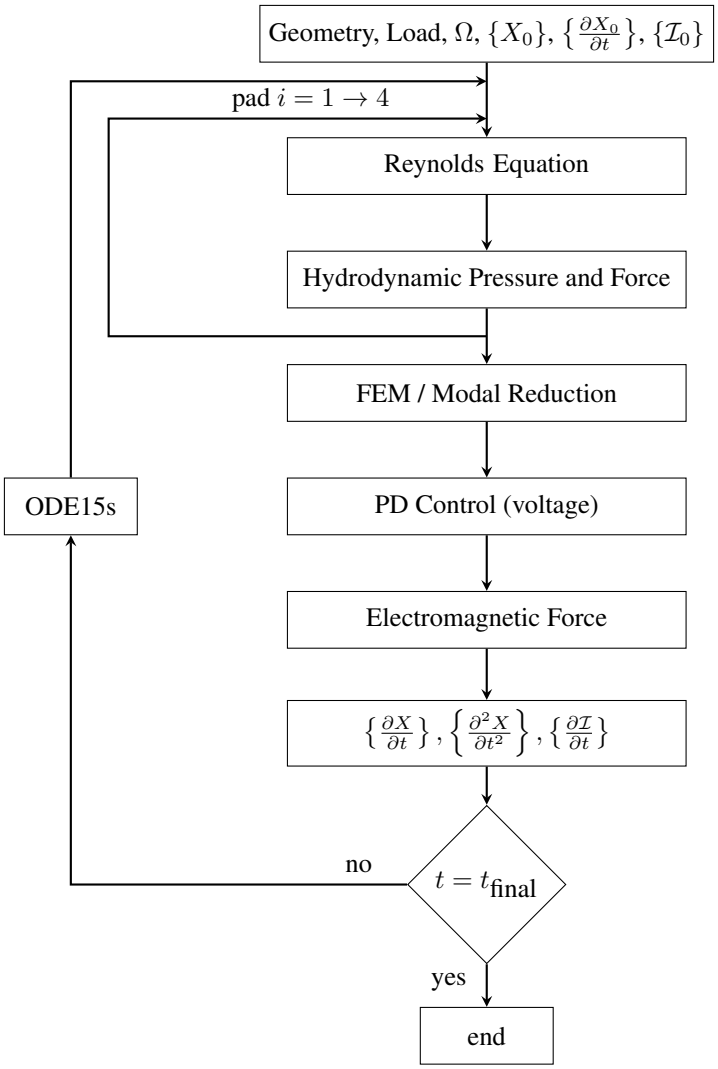

Figure 4. Flow chart of the algorithm used to simulate numerically the hydrodynamic bearing using flexible shaft with active pads.

7. use the equations of motion in Eq.(3) and Eq.(7) to calculate the higher order derivatives of the model;
8. if the current integration time is not equal to the final time t_{final}, the `ode15s` command continues the integration process, going back to step 2 in an iterative way. The higher order derivatives are used by the `ode15s` command to calculate the position $\{X\}$ of the system at a given time step t.

4. NUMERICAL RESULTS

The mathematical model is numerically integrated in time using the algorithm depicted in Fig. 4 and considering the parameter values listed in Table 1. These values refer to a rotor-bearing test rig at the Laboratory of Dynamics (EESC-USP). The adopted control strategy is the PD control, presented in Eq.(8).

In these analyses, the disk is subject to a mass imbalance caused by a localized mass positioned at a certain distance from the center of the disk, which can be mathematically expressed as follows:

$$\begin{aligned} F_Y^{unb} &= M_u d_u (2pi\Omega)^2 sin(2pi\Omega T) \\ F_X^{unb} &= M_u d_u (2pi\Omega)^2 cos(2pi\Omega T) \end{aligned} \tag{9}$$

where M_u is the mass of the imbalance and d_u is the distance from the mass to the center of the disk.

In this initial analysis, we will examine the scenario where displacement and velocity measurements are taken at the bearing to control the vibration amplitude at that location. However, we will also observe the influence of this control on the vibration amplitude at the node where the disk is located. We have chosen the values of 10^7 V.m^{-1} and 10^3 V.s.m^{-1} for the proportional and derivative gains in XY direction, respectively. These values were determined through trial-and-error to optimize the control effect (vibration attenuation) while ensuring that they do not exceed the ±10 V limits of

Table 1. Parameters of system used in the numerical simulations.

parameter	**value**	**unit**	**parameter**	**value**	**unit**
radial clearance (h_o)	100	μm	shaft length (L_s)	1	m
rotor radius (R)	40	mm	shaft mass (m_s)	2.242	kg
pad inner radius (R_s)	40.2	mm	shaft radius (R_s)	10	mm
pad thickness(h_s)	7	mm	disk radius (R_d)	100	mm
pad aperture angle	80	degree	distance to disk (L_d)	0.5	m
pad width	60	mm	disk mass (m_d)	3	kg
pad moment of inertia (I_s)	0.00016	kg.m^2	disk thickness (h_d)	6	mm
pad pivot position (φ)	0 / 90 / 180 / 270	degree	parameter a_0	6.5×10^{-3}	—
oil viscosity (μ)	0.032	N.s.m^{-2}	parameter b_1	0.12	H
preload factor	0.5	—	parameter b_0	4.7	Ω

the output ports in the acquisition system. We also have employed the same control gains for different rotation values to observe the influence of increased rotation on the system. This results in a greater mass imbalance and subsequently reduces the electromagnetic force that the actuator can provide to the system.

Initially, the hydrodynamic tilting pad journal bearing operates without the control system activated, allowing the rotor to exhibit its orbit with the known mass imbalance. After a time interval of two and a half seconds, the control loop is activated for an equal duration. During this time, the actuators adjust the position of the flexible shaft to the equilibrium position it would have if there were no mass imbalance in the system. The desired equilibrium position was determined through a simulation conducted under the assumption of no disturbance caused by the mass imbalance.

The Fig.(4(a),(c),(e)) represent the dynamic behavior of the shaft located at the bearing node for rotating speed of 600, 1800, and 3000 rpm. Initially, with the control system turned off, the blue curve represent the orbit of the rotating system due to mass imbalance. This curve represents the vibration amplitude of the system without control intervention. After a certain period of time, the control loop is activated and starts to act on the system. The effect of this intervention can be observed in the red line of the graph, which represents the new orbit of the shaft. It is noteworthy that the vibration amplitude has been significantly reduced compared to the initial condition, indicating the effectiveness of the control in reducing unwanted oscillations.

In the Fig.(4(b),(d),(f)), the same procedure mentioned earlier is performed, but now the dynamic behavior at the disk node is observed, aiming to analyze the influence of measurement and actuation at the bearing on the disk's orbit. For the case where the rotational speed of the system is 600 rpm(Fig.(4(b)), there is a slight reduction in the system's vibration amplitude when the controller is activated. This is due to the higher actuation force of the system and the actuation frequency being lower than the natural frequency of the system. Analyzing the case for a rotational speed of 1800 rpm (Fig.(4(d)), it is observed that the oscillation amplitude increased compared to the case where the control was turned off. In this specific case, the actuation frequency is above the natural frequency of the system, which is approximately 21.08 Hz. For a rotate speed of 3000 rpm (Fig.(4(f)), the reduction in amplitude was nearly negligible. In addition, there is a greater difficulty in controlling the amplitude at the disk node due to the control method being simple and not taking into account the dynamic of the rotating system. The electromagnetic actuator exhibits reduced actuation force and a certain delay for this frequency operating range.

In the second analysis, the measurement of the vibration amplitude and the control of the orbit caused by the mass imbalance will be performed at the node of the disk. The same procedure described earlier will be followed, with the control system turned off for a certain interval of time and then turned on for the same interval of time. The orbits will be analyzed at both the disk node and the bearing node.

In the present analysis, we have selected the values of 10^1 V.m^{-1} and 10^1 V.s.m^{-1} as the proportional and derivative gains in the XY direction, respectively. These values were carefully determined through an iterative process to maximize the control effect of vibration attenuation while ensuring that they remain within the ±10 V limits of the output ports in the acquisition system. Since the measurement is taken on the disk while the control is applied at the bearing, the controller gains have been significantly reduced due to the dynamics of the flexible shaft. Additionally, we have applied the same control gains for various rotational speeds to examine the impact of increased rotation on the system.

In the Fig.(6 (b),(d),(f)) illustrates the dynamic behavior of the rotating system for different rotational speeds, with vibration amplitude measurement taken at the disk. It can be observed that the reduction in amplitude when the control system is activated is insignificant. This is due to the simplicity of the controller, which does not take into account the dynamics of the flexible shaft.

Analyzing the Fig.(6 (a),(c),(e)), which represents the vibration orbit within the bearing, it is noticeable that when the controller is activated, the system exhibits small oscillations. However, the overall shape of the orbit remains similar to when the controller is deactivated. The reduction in amplitude is not as pronounced compared to the previous case study,

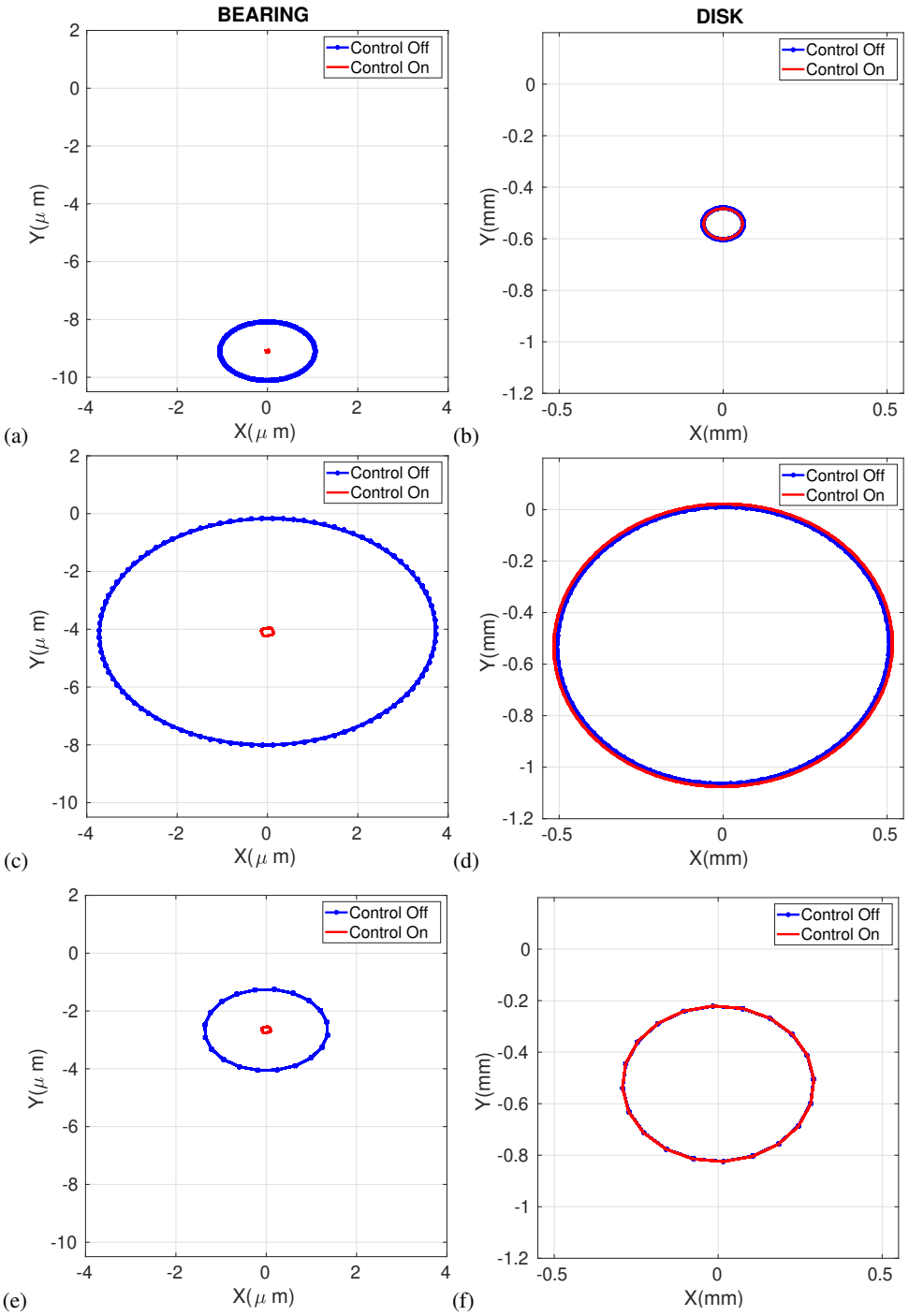

Figure 5. The position of a rotor with an unbalanced mass with measurements taken on the bearing: (a) the rotor's response at the bearing node (600 rpm), (b) the rotor's response at the disk node (600 rpm), (c) the rotor's response at the bearing node (1800 rpm), (d) the rotor's response at the disk node (1800 rpm), (e) the rotor's response at the bearing node (3000 rpm), (f) the rotor's response at the disk node (3000 rpm)

as the main objective of the second case study is to control the vibration amplitude at the disk.

5. CONCLUSION

In this work, the mathematical model of a tilting pad journal bearing with active pads was presented. A Proportional-Derivative controller was applied to control the movements of a flexible shaft with a central disk. This control is performed through electromagnetic actuators located behind the pads, and the dynamic behavior of the actuators was obtained

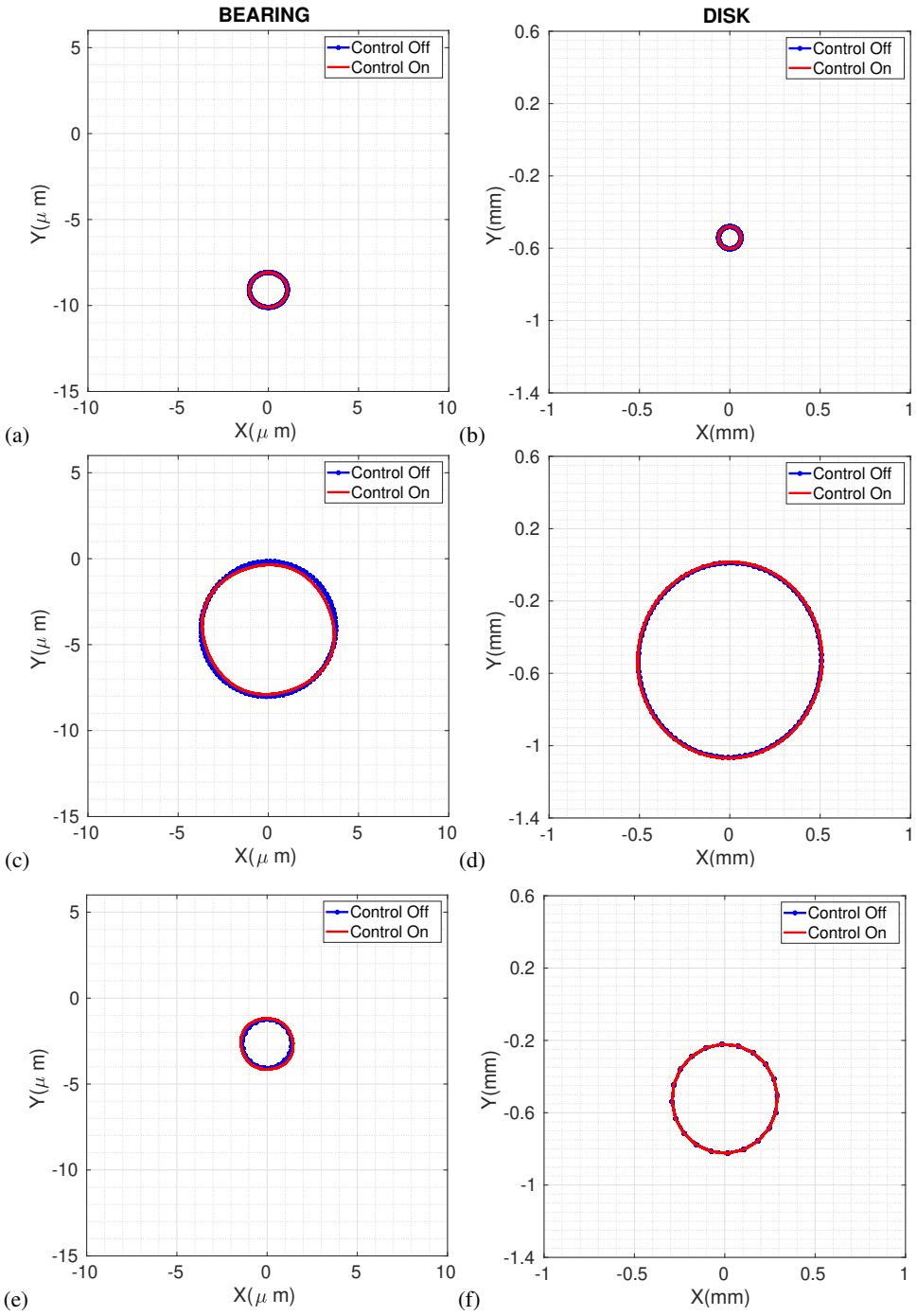

Figure 6. The position of a rotor with an unbalanced mass with measurements taken on the disk: (a) the rotor's response at the bearing node (600 rpm), (b) the rotor's response at the disk node (600 rpm), (c) the rotor's response at the bearing node (1800 rpm), (d) the rotor's response at the disk node (1800 rpm), (e) the rotor's response at the bearing node (3000 rpm), (f) the rotor's response at the disk node (3000 rpm)

through experimental measurements of the electromagnetic force generated by the actuator within a specific frequency range.

For the first case study, where the measurement was taken at the bearing, the Proportional-Derivative controller exhibited a significant reduction in vibration amplitude at that location. However, when observing the region where the disk is located, the reduction in amplitude was smaller due to the flexible nature of the shaft, which can exhibit different behavior from its end.

Now, analyzing the second case study, where the measurement is taken at the node of the disk, the vibration amplitude shows a relatively insignificant reduction. This is because the Proportional-Derivative control system is simplistic and

does not take into account the dynamics of the shaft when attenuating vibration at the bearing.

It is observed that as the system's rotational speed increases, the mass imbalance force has a greater influence on the system, resulting in higher vibration amplitudes. Furthermore, as the actuator's operating frequency increases, its electromagnetic force applied to the pad decreases, and there is a delay in its response due to the phase variation of the actuator.

Therefore, for future projects, it will be necessary to study other control techniques that can consider the dynamics of this long flexible shaft with a centered disk in order to achieve a significant reduction in the vibration amplitude of the system.

6. ACKNOWLEDGEMENTS

The authors acknowledge the support given to this project by FAPESP (Fundação de Amparo à Pesquisa do Estado de São Paulo), grant no. 2019/23220-2, CAPES (Coordenação de Aperfeiçoamento de Pessoal de Nível Superior), grant no. 88887.465094/2019-00, and CNPq (Coordenação Nacional de Desenvolvimento Científico e Tecnológico), under grant no. 301118/2018-3

7. REFERENCES

Bleuler, H., Cole, M., Keogh, P., Larsonneur, R., Maslen, E., Okada, Y., Schweitzer, G., Traxler, A. *et al.*, 2009. *Magnetic bearings: theory, design, and application to rotating machinery*. Springer Science & Business Media.

Hamrock, B.J., Schmid, S.R. and Jacobson, B.O., 2004. *Fundamentals of fluid film lubrication*. McGraw-Hill Co., New York.

Moraes, D.C. and Nicoletti, R., 2010. "Hydrodynamic bearing with electromagnetic actuators: Rotor vibration control and limitations". In *Proceedings of ISMA 2010—International Conference on Noise and Vibration Engineering, Leuven, Belgium, September*. pp. 20–22.

Nelson, H.D. and McVaugh, J.M., 1976. "The Dynamics of Rotor-Bearing Systems Using Finite Elements". *Journal of Engineering for Industry*, Vol. 98, No. 2, pp. 593–600. ISSN 0022-0817. doi:10.1115/1.3438942. URL `https://doi.org/10.1115/1.3438942`.

Nicoletti, R., 2003. *Mancais segmentados com lubrificação ativa: teoria, experimento e aplicação*. Ph.D. thesis, Universidade Estadual de Campinas, Faculdade de Engenharia Mecanica, Campinas, SP. URL `https://doi.org/10.47749/T/UNICAMP.2003.281906`.

Nicoletti, R., 2013. *Estudo do controle ativo e passivo de vibrações em sistemas rotativos e estruturais*. Ph.D. thesis, Universidade de São Paulo.

Pereira da Silva, H. and Nicoletti, R., 2021. "Rotor vibration control using hydrodynamic bearing with active pads". doi:10.26678/ABCM.COBEM2021.COB2021-0067.

Pizarro Viveros, H. and Nicoletti, R., 2014. "Lateral vibration attenuation of shafts supported by tilting-pad journal bearing with embedded electromagnetic actuators". *Journal of engineering for gas turbines and power*, Vol. 136, No. 4.

Russo, F.H., 1998. *Identificação das propriedades dinâmicas de mancais segmentados híbridos: teoria e experimento*. Master's thesis.

Shampine, L.F. and Reichelt, M.W., 1997. "The matlab ode suite". *SIAM Journal on Scientific Computing*, Vol. 18, pp. 1–22.

8. RESPONSIBILITY NOTICE

The authors are solely responsible for the printed material included in this paper.